Response to Reviewer 1

Question 1: Generality Across Waveforms and Environments

In Section 5 the authors acknowledge that this is a pilot study and explicitly discuss the limitation to LFM, 0.5° scans, but they have not provided any new empirical tests on NLFM waveforms, different elevation angles, or varied sea conditions. They must either include at least one additional validation case (e.g., an NLFM scan or a different elevation/season) or explicitly narrow all claims to the current test setup.

We agree with the reviewer's comment. To demonstrate the applicability of the HSCI algorithm in other scenarios, we have added a case using the NLFM waveform (Figures 11c and 11d) in the revised manuscript. This case was observed only one minute apart from the LFM waveform case shown in Figures 11a and 11b. A comparison of the reflectivity after ship clutter suppression reveals similar results, indicating that the HSCI algorithm maintains robust performance even under the NLFM waveform. The specific revisions can be found in Section 4.1 (Line 343 highlighted content).

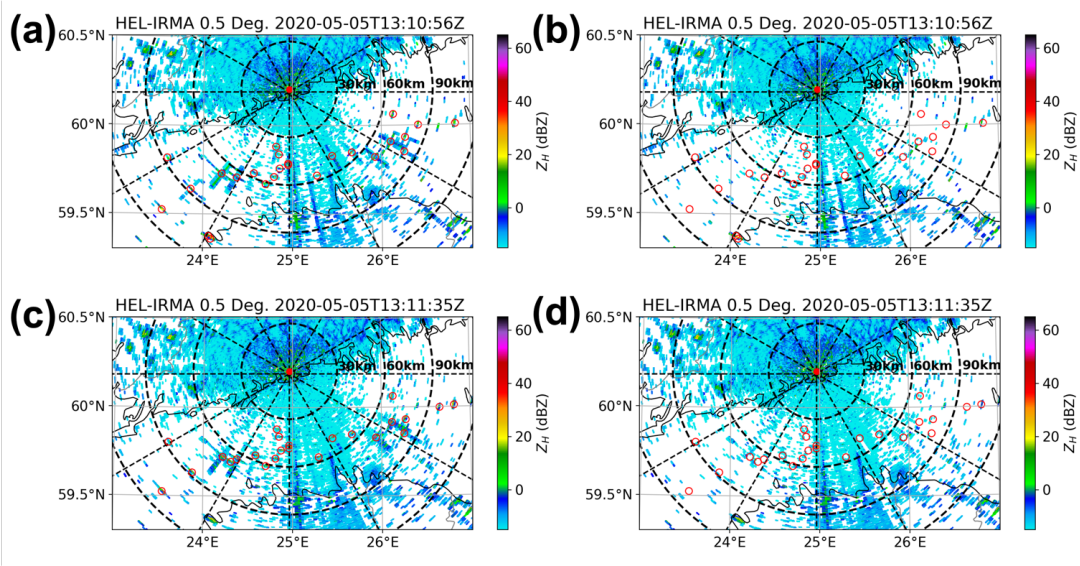

Figure 11. Reflectivity on 0.5° elevation of Kumpula radar using LFM (1310 UTC) and NLFM (1311 UTC) waveforms on 5 May 2020. (a) Before ship clutter filtering using LFM waveform; (b) After ship clutter filtering using LFM waveform; (c) Before ship clutter filtering using NLFM waveform; (d) After ship clutter filtering using NLFM waveform. The mainlobe identification results are highlighted by red circles.

The occurrence of super-refraction which is conductive to ship clutter signatures has seasonal dependence (Lopez, 2009). Usually, ship clutter signatures are more common in summer than in winter. We have looked through our observations in the winter of 2020, but identified very limited ship clutter cases in precipitation. We found a single case where ship clutter was mixed with precipitation, with just one ship clutter present across the entire PPI. Fortunately, the HSCI algorithm successfully detected and filtered this ship clutter without excessively suppressing the surrounding precipitation echoes. Further clarification on this point has been added in DATA section of the manuscript (Line 126; highlighted content).

Lopez, P. (2009). A 5-yr 40-km-resolution global climatology of superrefraction for ground-based weather radars. Journal of applied meteorology and climatology, 48(1), 89-110.

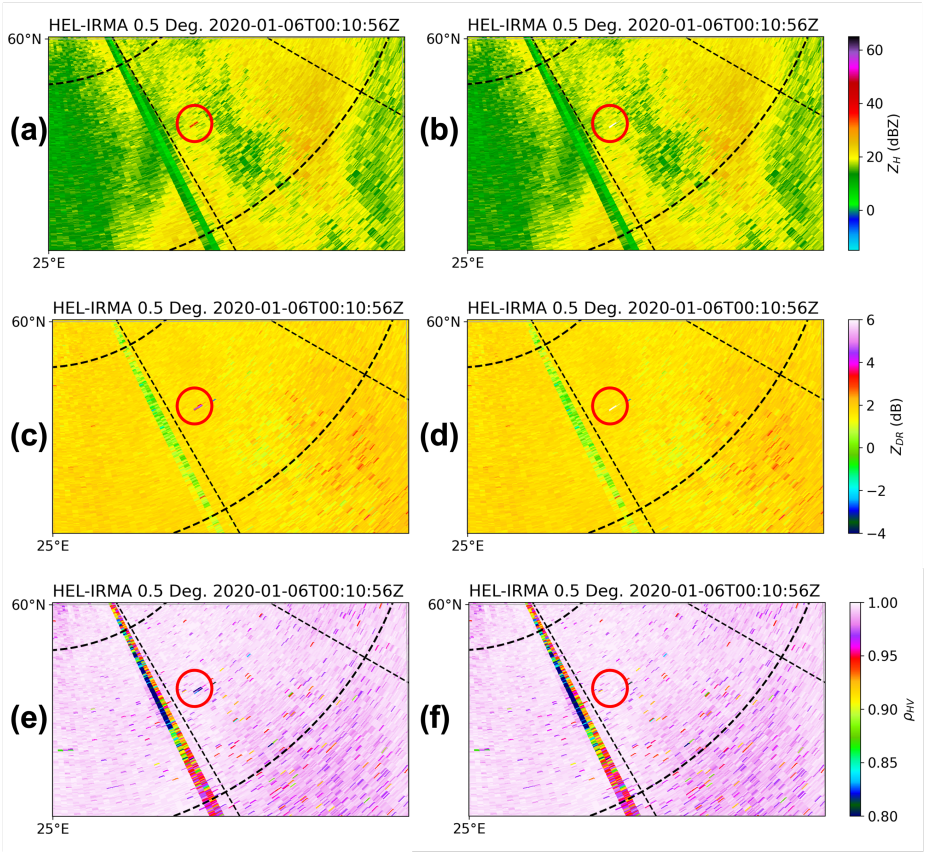

Figure xxx: 0.5° elevation of Kumpula radar using LFM waveform at 0010 UTC 6 Jau 2020. (a) Reflectivity before ship clutter filtering; (b) Reflectivity after ship clutter filtering; (c) Differential reflectivity before ship clutter filtering; (d) Differential reflectivity after ship clutter filtering; (e) Correlation coefficient before ship clutter filtering; (f) Correlation coefficient after ship clutter filtering.

Although additional content has been included to help demonstrate that the applicability of the HSCI algorithm is not limited to a specific observational scenario, the authors still believe that the current study has not sufficiently validated the full extent of the algorithm's applicability. Therefore, the discussion of the algorithm's limitations has been further emphasized in Section 5 of the manuscript (Line 343 highlighted content). The specific content is as follows:

Due to the limitations of available observational data, this study develops and evaluates the HSCI algorithm primarily based on ship clutter observed by the Kumpula radar in the Gulf of Finland, using an LFM waveform. While the features designed for ship clutter identification and the overall logic of the HSCI algorithm are intended to be general and not tied to a specific radar system or waveform, we acknowledge that the current validation is restricted to a single radar platform, geographic location, sea state, and waveform configuration. Therefore, the robustness and generalizability of the algorithm under varying conditions—such as across different radar systems, geographical regions, environmental conditions (e.g., sea clutter dynamics influenced by wind or temperature), seasons, and transmitted waveforms—remain to be comprehensively assessed. We recognize this as a significant limitation of the present work. Future studies will aim to address this issue by applying the HSCI algorithm to a broader range of observational datasets, enabling a more rigorous evaluation of its performance and adaptability in diverse operational scenarios.

Question 2: Manual Labeling Bias

The authors clarified that a single annotator (the first author) labeled all gates with continuity checks, improving transparency in Section 2, but they still provide no inter-annotator agreement statistics. To address potential subjectivity, they should perform a simple second-annotator check on a representative subset or, at minimum, discuss in more depth how annotation bias might affect results.

We agree with the reviewer's suggestion. To further demonstrate the reliability of the dataset selection, the second author of this manuscript conducted a secondary annotation on 170 ship clutter cases from

10 scans, which were selected from the entire dataset (comprising 1,600 ship clutter cases across 110 scans). The results show that only two relatively weak ship clutter showed ambiguity, indicating that the overall annotation quality is high and that potential subjectivity has a limited impact on the dataset. The specific revisions can be found in Section 2 (Line 123 highlighted content).

Question 3: Quantitative Assessment of Precipitation-Loss

The manuscript now shows qualitative rain-field improvements in mixed scenes (Fig. 13b), but it lacks any numeric metric on how many precipitation gates are inadvertently removed. The authors need to report concise quantitative statistics (for example, the percentage of precipitation gates masked) for at least one mixed-scene case.

We agree with the reviewer's suggestion. In the revised manuscript, we replaced the original Figure 12 with a more informative case, in which several ship clutter events were completely mixed with precipitation echoes. This new case includes the three main output scenarios of the HSCI algorithm: (1) ship clutter is successfully identified (highlighted with red or white circles); (2) precipitation echoes are mistakenly identified as ship clutter (red or white circles indicated by arrows); and (3) ship clutter is not effectively identified (highlighted with black rectangles). The reviewer emphasized the second scenario. In this scenario, although errors occurred in the mainlobe identification, the application of velocity and SNR filters in sidelobe identification effectively controlled the loss of precipitation echoes—that is, only the range gate misidentified as a ship clutter mainlobe and its eight nearest neighboring gates were mistakenly removed. The specific revisions can be found in Section 4.1 (Line 343 highlighted content).

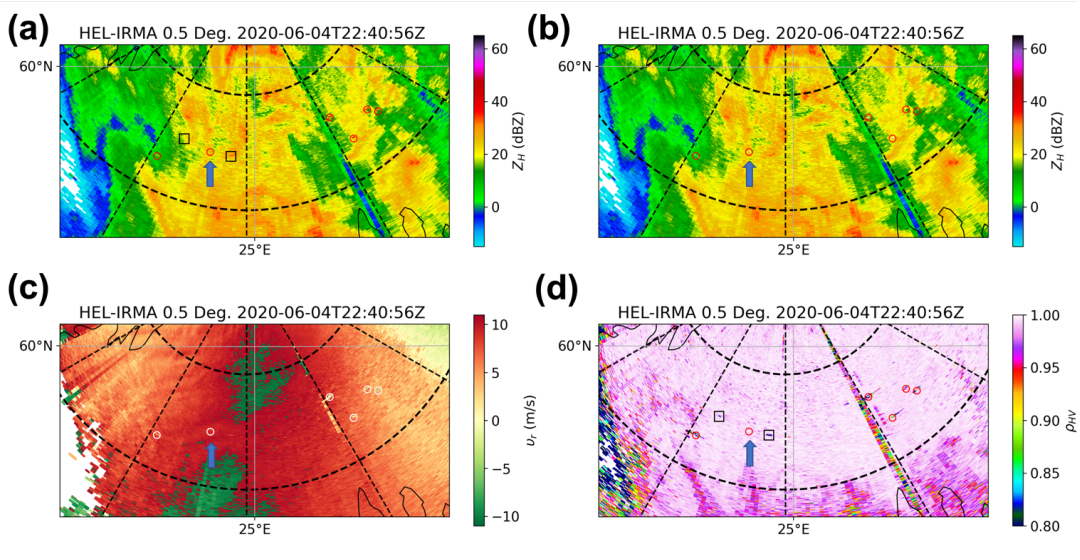

Figure 12: 0.5° elevation of Kumpula radar using LFM waveform at 2240 UTC 4 June 2020. (a) Reflectivity before ship clutter filtering; (b) Reflectivity after ship clutter filtering; (c) Doppler velocity before ship clutter filtering; (d) co-polar correlation coefficient after ship clutter filtering. The mainlobe identification results are highlighted with red or white circles, with misidentified cases indicated by blue arrows, while the unrecognized ones are highlighted with black rectangles.

Question 4: Independent Test Dataset

The authors document using 5-fold GridSearchCV in Section 3.1.3, but they did not reserve any fully independent radar volume or day as a hold-out test. They should, if feasible, reserve one full sweep or day for independent validation and report its performance.

We agree with the reviewer's suggestion. We used radar data from the same day (4 June) as that analyzed in Figure 13 for validation. We extracted 24 scans, selecting one scan per hour, and determined the locations of ship clutter using the same method as employed for dataset selection (described in Section 2). The evaluation results are summarized in Table 5. A total of 247 ship clutter events were identified across the 24 scans (i.e., the sum of the second and third columns in the second row). Of these, the HSCI

algorithm successfully detected 238, missing only 9. Additionally, 31 range gates associated with precipitation echoes were mistakenly identified as ship clutter. However, as discussed in the Question 3, the actual loss of precipitation echoes is well controlled, thanks to the velocity and SNR thresholds integrated into the HSCI algorithm. The specific revisions can be found in Section 4.2 (Line 426 highlighted content).

Table 5: Performance evaluation results of HSCI algorithm for identifying ship clutter mainlobe based on observations from 4 June 2020.

Time (UTC)	Hit	Miss	False Alarm
Total	238	9	31
00:00:41	21	0	2
01:00:40	14	0	2
02:00:40	10	1	4
03:00:41	11	1	7
04:00:40	14	0	2
05:00:40	12	1	0
06:00:41	8	0	1
07:00:40	9	0	2
08:00:40	7	1	0
09:00:41	4	0	0
10:00:41	2	0	1
11:00:41	6	1	1
12:00:41	10	1	0
13:00:41	16	0	3
14:00:40	14	0	2
15:00:40	16	0	0
16:00:40	11	0	0
17:00:41	8	1	0
18:00:41	12	0	2
19:00:40	10	0	1
20:00:41	11	0	0
21:00:41	4	0	0
22:00:41	6	1	1
23:00:40	2	1	0